J|A|C|S

A R T I C L E S

Monolayers of Twisted Binaphthyls for Aromatic Crystallization at Low Nucleation Densities and High Growth Rates

Sang-Mi Jeong and Ji-Woong Park*

Department of Materials Science and Engineering, Gwangju Institute of Science and Technology, 1 Oryong-dong, Buk-gu, Gwangju 500-712, Korea

Received September 20, 2007; Revised Manuscript Received January 10, 2008; E-mail: jiwoong@gist.ac.kr

Abstract: Monolayers of 1,1′-bi-2-naphthol (BN) derivatives, of which the two naphthalene rings are twisted along the carbon(1)−carbon(1′) single bond, were studied for their conformational effect on the growth of pentacene crystals on their monolayer surface. BN monolayers with H and Br at 6,6′-positions (H-BN and Br-BN) were prepared by immersion-coating in toluene solution of the corresponding $BNSiCl_2$. Pentacene was thermally evaporated onto the H-BN and Br-BN monolayers, silica, octadecylsilyl (ODTS) SAM, and a micropattern of H-BN and ODTS SAM. Pentacene crystals were also grown on the SAMs of 1-naphthylsilyl-(NPh), phenylsilyl(Ph), and diphenylsilyl (DPh) groups, which are aromatic and have contact angle values similar to those of the the BN monolayers. AFM images of the crystals at the early stage of growth indicated that the BN monolayers suppressed the nucleation while facilitating the growth of nuclei to larger crystals. The low nucleation density and high growth rate are accounted for by the amorphous nature of the twisted BN monolayer surface where the intermolecular interaction between neighboring adsorbates is likely to be suppressed. The results offer new insights into designing surfaces for controlling the crystallization kinetics of organic materials.

Introduction

Controlling the assembly of organic molecules is essential for the development of high efficiency functional devices based on organic thin films.[1,2] While control over morphology, position, orientation, and patterning of organic crystals on the substrate surface still remains a challenge, significant progress has been made by several recent studies utilizing self-assembled monolayers (SAMs) of various functionalities and/or surface patterns as crystallization templates.[3−8]

In general kinetic models of crystallization, the favorable volume free energy associated with the formation of a crystal and the interfacial energy penalty associated with the phase boundary created by the crystal sum to the total free energy of crystallization as a function of its size, which defines the activation barrier to be overcome in order for a nucleus of critical size to form and grow further.[9] Because of high activation barrier

of homogeneous nucleation, most crystallization occurs via heterogeneous nucleation; i.e., the crystals grow from the nuclei that formed on the surface of a foreign substance, and thus a straightforward approach to controlling crystallization relies on chemical modification of the interaction between crystallizing molecules and a nucleation substrate surface.[9−11]

An ideal substrate surface for growing organic crystals for thin film devices is the one where the crystals can grow at as low a nucleation density and high a growth rate as possible so as to ultimately produce a nearly single crystalline film.[1] To the best of our knowledge, such a surface has not been reported. Crystal growth is usually slow on the surface inhibiting nucleation, such as fluoroalkyl SAMs.[7] Here we demonstrate a new type of surface consisting of the monolayers of 1,1′-binaphthyl, a twisted biaryl compound, which suppresses the nucleation of aromatic crystals but facilitates the growth of their nuclei that already formed. The results offer new insights into designing surfaces for controlling the crystallization kinetics of organic materials.

Our approach is based on the assumption that, in order for the nuclei to form via heterogeneous nucleation mechanism, the substrate surface needs to provide an environment in which the molecules meet in an arrangement similar to that in its

(1) Dimitrakopoulos, C. D.; Malenfant, P. R. L. *Adv. Mater.* **2002**, *14*, 99−117.
(2) Singh, T. B.; Sariciftci, N. S. *Annu. Rev. Mater. Res.* **2006**, *36*, 199−230.
(3) Briseno, A. L.; Aizenberg, J.; Han, Y. J.; Penkala, R. A.; Moon, H.; Lovinger, A. J.; Kloc, C.; Bao, Z. A. *J. Am. Chem. Soc.* **2005**, *127*, 12164−12165.
(4) Briseno, A. L.; Mannsfeld, S. C. B.; Ling, M. M.; Liu, S. H.; Tseng, R. J.; Reese, C.; Roberts, M. E.; Yang, Y.; Wudl, F.; Bao, Z. N. *Nature* **2006**, *444*, 913−917.
(5) Hiremath, R.; Varney, S. I.; Swift, J. A. *Chem. Mater.* **2004**, *16*, 4948−4954.
(6) Wilkinson, F. S.; Norwood, R. F.; McLellan, J. M.; Lawson, L. R.; Patrick, D. L. *J. Am. Chem. Soc.* **2006**, *128*, 16468−16469.
(7) Steudel, S.; Janssen, D.; Verlaak, S.; Genoe, J.; Heremans, P. *Appl. Phys. Lett.* **2004**, *85*, 5550−5552.
(8) Cox, J. R.; Ferris, L. A.; Thalladi, V. R. *Angew. Chem., Int. Ed.* **2007**, *46*, 4333−4336.
(9) Ward, M. D. *Chem. Rev.* **2001**, *101*, 1697−1725.
(10) Ruiz, R.; Choudhary, D.; Nickel, B.; Toccoli, T.; Chang, K. C.; Mayer, A. C.; Clancy, P.; Blakely, J. M.; Headrick, R. L.; Iannotta, S.; Malliaras, G. G. *Chem. Mater.* **2004**, *16*, 4497−4508.
(11) Wang, W. C.; Zhong, D. Y.; Zhu, J.; Kalischewski, F.; Dou, R. F.; Wedeking, K.; Wang, Y.; Heuer, A.; Fuchs, H.; Erker, G.; Chi, L. F. *Phys. Rev. Lett.* **2007**, *98*, 225504.
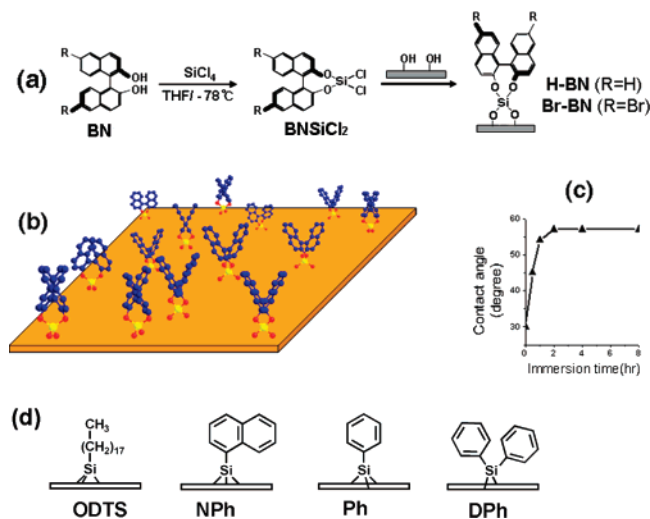
Figure 1. Synthesis and structure of 1,1′-binaphthyls(BN) monolayers and various SAMs: (a) synthetic scheme of BN monolayers; (b) sketch of amorphous surface by randomly oriented BNs in the monolayer; (c) water contact angle on the H-BN monolayer coated on the silica surface as a function of immersion time in toluene solutions of H-BNSiCl$_2$; (d) chemical structures of ODTS, NPh, Ph, and DPh SAMs whose nucleation effect was investigated in comparison with that of BN monolayers.

crystalline state. Prior to the formation of the nuclei which consist of several molecules,[12] the molecules will adsorb and diffuse onto the surface as in the case of atomic crystallization.[13] If the molecules to be crystallized are adsorbed onto the surface in a random orientation relative to neighboring ones in a way that is far different from their crystalline arrangement, formation of a nucleus from these molecules may be kinetically hindered.

We create a new surface to induce such a disordered molecular arrangement from an aromatic compound, 1,1′-bi-2-naphthol (BN) (Figure 1), which has two naphthalene rings connected by a C(1)−C(1′) single bond about which the two rings are twisted.[14] As the BN molecules bind to the surface by the 2,2′ bridge as illustrated in Figure 1a, the BNs give an amorphous surface where the naphthalene rings are randomly oriented without lateral order because of their rigid, twisted, asymmetric shape. As flat aromatic molecules which can make a $\pi-\pi$ interaction with the naphthalene rings are evaporated onto the BN monolayer surface, they will be randomly adsorbed onto the surface until their crystallization takes places.

To investigate the conformational effect of the BN monolayer on organic crystallization, we utilized pentacene whose crystallization has been studied intensively in recent years as a model molecule among organic semiconductors.[10,15−17] Pentacene thin films are known to grow by the diffusion-mediated process in which monomers diffuse initially on a bare substrate, and when a critical number of them meet a stable nucleus is formed.[12] The crystal structure of bulk pentacene layers consist of layers of pentacene molecules arranged in a herringbone packing motif

(12) Ruiz, R.; Nickel, B.; Koch, N.; Feldman, L. C.; Haglund, R. F.; Kahn, A.; Family, F.; Scoles, G. *Phys. Rev. Lett.* **2003**, *91*, 136102.
(13) Zhang, Z. Y.; Lagally, M. G. *Science* **1997**, *276*, 377−383.
(14) Park, J. W.; Ediger, M. D.; Green, M. M. *J. Am. Chem. Soc.* **2001**, *123*, 49−56.
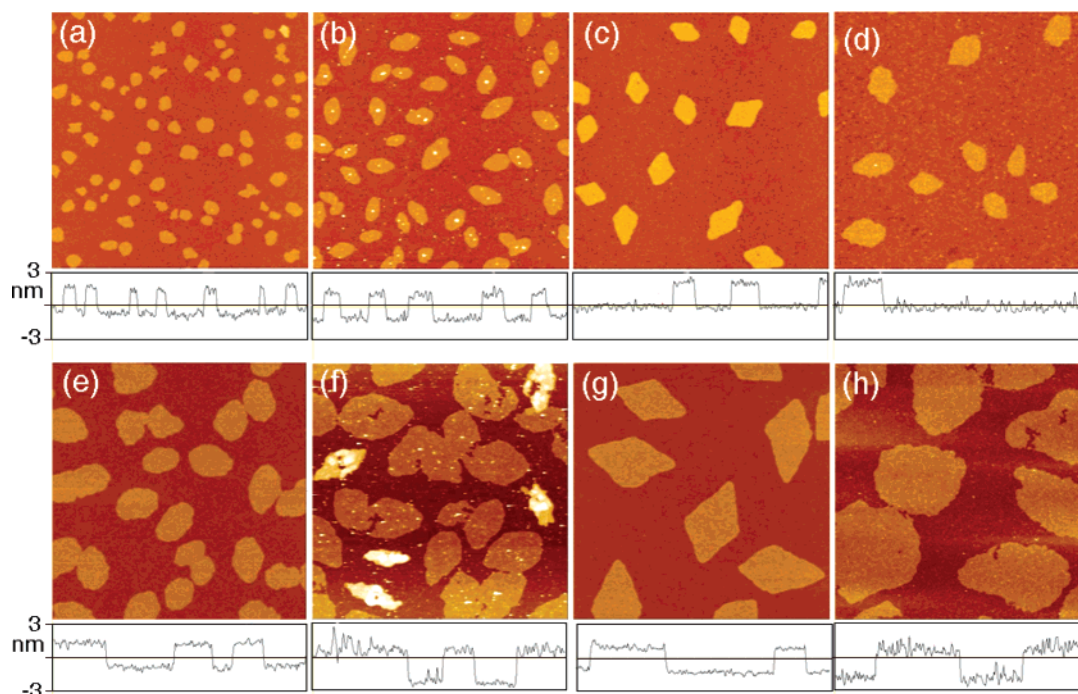(15) Heringdorf, F.; Reuter, M. C.; Tromp, R. M. *Nature* **2001**, *412*, 517−520.
(16) Yang, H. C.; Shin, T. J.; Ling, M. M.; Cho, K.; Ryu, C. Y.; Bao, Z. N. *J. Am. Chem. Soc.* **2005**, *127*, 11542−11543.
(17) Drummy, L. F.; Martin, D. C. *Adv. Mater.* **2005**, *17*, 903−907.

Table 1. Water Contact Angle Data (deg) for Various SAMs and the Silica Surface Investigated

	silica	H-BN	Br-BN	NPh	Ph	DPh	ODTS
contact angle	30 ± 2	51 ± 3	56 ± 2	60 ± 3	62 ± 3	57 ± 3	90 ± 5

with an interlayer spacing of $d_{001} = 14.1$ Å. In thin film phases the d_{001} value of multilayer crystals is about 15 Å.[18]

Results and Discussion

The BNs were reacted with an equimolar amount of SiCl$_4$ and triethylamine in THF to yield BNSiCl$_2$, as shown in Figure 1. The monolayers were obtained by immersion of silica substrates in dilute toluene solutions of BNSiCl$_2$ of a concentration 0.1 mg/mL. Residual volatile reactants and any insoluble solid such as amine salts were removed by several steps so as to minimize contamination of the monolayer-coated surface. We could obtain smooth surfaces with root-mean-square roughness of below 0.3 nm (Supporting Information) by employing a minimum immersion time of 1 h which was determined by contact angle measurement and atomic force microscopy for the samples from different immersion times (Figure 1c). The BN monolayer surface is rough only on the molecular level and can be regarded as a field of *molecular hedgehogs*.

To draw distinction between the conformational effect and the surface energy effect of the SAM surface, the SAMs of octadecylsilyl (ODTS) group and other aromatic compounds such as 1-naphthylsilyl (NPh), phenylsilyl (Ph), and diphenylsilyl (DPh) groups, which exhibited water contact angle values similar to the BNs (Table 1), were prepared and used as crystallizing substrates.

Pentacene was thermally evaporated onto the SAM-coated silica substrates, and for comparison it was also evaporated onto bare silica and ODTS SAM-coated silica substrates, which have been used as the substrate for organic crystal growth in much of the literature. Small pieces of the substrates were placed side by side in the evaporation chamber to exclude any effect of nonuniform flux inside the chamber. The substrates were maintained at room temperature. To see the early stage nucleation behavior, the deposition rate was adjusted to small values near 1 Å/min.[19] Samples with different coverage were obtained by varying the evaporation time while monitoring the thickness indicator inside the evaporation chamber. Pentacene was also evaporated onto a micropatterned surface consisting of alternating stripes of the ODTS SAM and BN monolayer, which was prepared via microcontact printing of ODTS onto the silica substrate followed by immersion-coating in a BNSiCl$_2$ solution.

To optimize the crystallization conditions suitable for study of the early stage of crystal growth, we first investigated the growth of pentacene crystal on the silica and ODTS SAM surface while comparing with that on the BN monolayer. The resulting pentacene submonolayers were imaged on the tapping mode atomic force microscope (AFM) as presented in Figure 2. The images clearly show that the number of crystals grown on the BN monolayer surface is lower than those on the other surfaces while their size on the BN monolayer is larger.

(18) Fritz, S. E.; Martin, S. M.; Frisbie, C. D.; Ward, M. D.; Toney, M. F. *J. Am. Chem. Soc.* **2004**, *126*, 4084−4085.
(19) The gauge thickness divided by the deposition time varied by 0.5−2.0 Å/min under the same voltage setting of evaporator.

Figure 2. Height contrast AFM images of pentacene submonolayers grown on various substrate surfaces: (a, e) silica; (b, f) ODTS; (c, g) H-BN; (d, h) Br-BN. The two sets of samples were obtained from two batches of pentacene evaporation differing in deposition time, which resulted in the difference in the coverage and the average island size between the two sets. Cross-sectional height profiles are given underneath each panel. Panel size: $5 \times 5 \ \mu m^2$.

Table 2. Nucleation Density (N) of the Pentacene Submonolayers Grown on Two Batches of Four Substrates in Figure 2[a]

	set 1 (a–d)			set 2 (e–h)		
	θ	$A(\theta)/\mu m^2$	$N/\mu m^{-2}$	θ	$A(\theta)/\mu m^2$	$N/\mu m^{-2}$
H-BN	0.10	0.16	0.63	0.32	0.84	0.38
Br-BN	0.14	0.20	0.70	0.53	1.88	0.28
silica	0.10	0.03	3.33	0.33	0.36	0.92
ODTS	0.20	0.12	1.67	0.51	0.52	0.98

[a] N was estimated by $\theta/A(\theta)$.

In the diffusion regime of the crystal growth, the kinetics of crystallization, characterized by the ratio of the diffusion constant D to the incoming flux F, determines the nucleation density (N),[10]

$$N = C(F/D)^\chi \cong \theta/A(\theta)$$

where the exponent χ is a positive number that is related to the critical island size, θ is the coverage, C is proportionality constant, and $A(\theta)$ is the average island size. Because each batch of pentacene evaporation has a specific flux that is determined by various experimental factors, the nucleation density (N) is system specific and therefore comparison of the crystallization behavior on various substrates must be done on each set of samples prepared from the same batch of evaporation.

The N values of the samples in Figure 2 were estimated by the above equation and listed in Table 2. Several batches of the samples differing in coverage indicated that the ratio of N values of the silica and ODTS surface to those of BN monolayers maintained in the range 2–10.

The values of θ, $A(\theta)$, and N of the pentacene crystals on the BN monolayer, obtained from the AFM images for smaller regions of 5×5 or $10 \times 10 \ \mu m^2$, were almost the same as those obtained from large area images by the field emission scanning electron microscope (FE-SEM) (Figure S8) as well as by AFM scanning over $30 \times 30 \ \mu m^2$ regions of the samples (Figures S7 and S8). Fluorescence optical microscope (FOM) images supported uniform distribution of the crystals over a large area although their image contrast was not sufficient for analysis. We estimated the N values for most of the samples from their AFM images for the sample areas of 5×5 or $10 \times 10 \ \mu m^2$.

The crystals grown by secondary nucleation on the surface of preformed monomolecular crystals or particle impurities were found in all of the images in a small portion (for example, Figure 2f). Contribution by the crystals with the parts of secondary growth to θ and $A(\theta)$ value was approximated using the surface coverage of the corresponding primary crystals underneath.

The crystals formed on the H-BN monolayer oftentimes exhibited a parallelepiped shape with thickness of 1.5–2.0 nm, approximately the same as the monomolecular length of pentacene, indicating that the crystal growth occurred selectively over lateral crystal planes.

The average island size, $A(\theta)$, of the crystals grown on the BN monolayers was usually the largest among those on the substrate surfaces investigated. The absence of irregular fractal geometry in the crystals grown on the BN monolayers and their large size suggest that the surface diffusion was not a limiting factor in the crystallization on the BN monolayer surface.

The different growth behaviors of the crystals on the BN monolayer surface as compared with other surfaces were evidently shown by the image of pentacene crystals grown on the patterned surface of the BN and ODTS (Figure 3). It is of particular interest that none of the crystals in the BN regions overgrew into the ODTS region across the boundary between the regions of the BN and ODTS SAMs. This also indicates
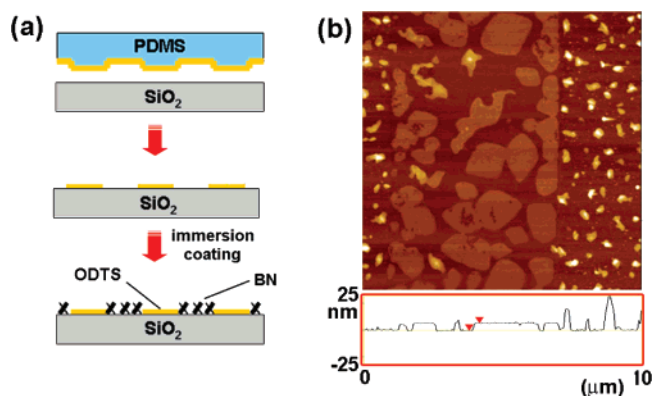
Figure 3. Growth of pentacene crystals on a BN/ODTS stripe pattern: (a) micropatterning of BN/ODTS SAM; (b) height contrast AFM image of pentacene crystals grown on the pattern.

that the growth rate of pentacene crystals on the BN monolayer is higher than that on the ODTS SAM surface.

We could not find any difference in the pentacene crystallization behaviors between the BN monolayers prepared from enantiomerically pure (R or S) or racemic 1,1′-BNs. This is reasonable considering that the pentacene molecules or their crystals do not contain any structural aspect of chirality.

Since the water contact angle values of H-BN and Br-BN monolayers fall between those of the hydrophilic silica and hydrophobic ODTS SAM surface, which showed higher nucleation density and smaller island size than the BN monolayers, it is unlikely that the crystallization behavior on the BN monolayers is related to the effect of the surface energy, which is frequently considered in explanation of nucleation density variation in organic crystallization.

To draw clear distinction between the conformational effect and surface energy effect, we compared the crystallization behavior on the BN monolayers with that on the SAMs of other aromatic compounds, which have very similar chemical structures as well as surface energies (contact angle values). In Figure 4 are shown the AFM images of the early stage pentacene crystals grown on the NPh, Ph, and DPh SAMs as compared with those on the H-BN monolayer and the silica surface (as a control). In Table 3 are listed θ, A(θ), and N values estimated from the AFM images in Figure 4.

In the images obtained from several batches of crystallization experiment including those in Figure 4, the pentacene crystals on the other aromatic SAMs did not show much difference from those on silica or ODTS SAM, whereas those on the BN monolayers consistently exhibited much lower nucleation densities and larger island sizes. In the particular set of images shown in Figure 4, the NPh SAM, which consists of monomeric naphthyl groups, gave an almost 10 times larger N value and a 15 times smaller $A(\theta)$ value than the H-BN monolayer. This result indicates that the unique crystallization behavior of pentacene on the BN monolayers was not caused either by the effect of the surface energy or the aromatic chemical structure itself, supporting that the effect was caused by the rigid, twisted conformation of the BN molecules in their SAMs.

The low nucleation density, the large island size, and the single crystallike morphology are all indicative of higher diffusion rates of the pentacene molecules adsorbed onto the BN monolayer surface. Our observation is consistent with the equation introduced above, which predicts that a low nucleation
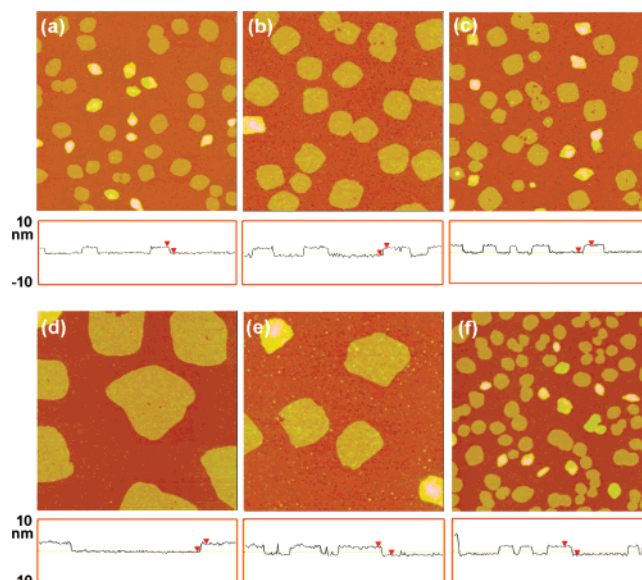
Figure 4. Height contrast AFM images of pentacene crystals grown on different aromatic SAM surfaces with similar water contact angle values: (a) NPh; (b) Ph; (c) DPh; (d) H-BN; (e) Br-BN; (f) silica (as a control). Cross-sectional height profiles are given under each panel. Panel size: $5 \times 5 \ \mu m^2$.

Table 3. Nucleation Density (N) of the Pentacene Crystals Grown on the SAMs of Various Aromatic Compounds

param	NPh	Ph	DPh	H-BN	Br-BN	silica
θ	0.21	0.34	0.25	0.38	0.16	0.33
$A(\theta)/\mu m^2$	0.12	0.35	0.15	1.89	1.37	0.09
$N/\mu m^{-2}$	1.84	0.96	1.68	0.20	0.12	3.80

density is obtained from a large diffusion constant at a constant flux.

The low nucleation density observed on the BN monolayer may be accounted for differently from that on the nonstick surfaces such as fluorinated SAMs in respect that while the adsorption of incoming molecules onto the BN surface is facilitated via their $\pi-\pi$ interaction with the naphthalene groups of the surface, the formation of nuclei is suppressed by the amorphous nature of the BN surface which can induce disordered arrangement of adsorbates. We postulate that many of the misaligned neighboring adsorbates exist in a monomeric form so as to readily diffuse and stick onto the growing crystals.

Conclusion

We have synthesized a new type of organic monolayer from twisted aromatic compounds, 1,1′-bi-2-naphthol (BN) derivatives, and demonstrated that crystallization of flat aromatic molecules on the amorphous monolayer of the BN molecules occurs at a low nucleation density and a high growth rate. The result is accounted for by the suppression of the crystallike molecular arrangement of the molecules adsorbed onto the BN monolayer surface in the diffusion regime of the crystallization kinetics. While further studies are needed to apply the new surface to the fabrication of organic devices, the concept demonstrated here may be exploited for controlled crystallization of organic molecules on the surface via combining with other methods of surface treatment.

Molecular Systems at the Gwangju Institute of Science and Technology in Korea.

JA077291X